A Dynamical Model for CSI Feedback in Mobile MIMO Systems using Dynamic Mode Decomposition

1st Fayad Haddad, 2nd Carsten Bockelmann, 3rd Armin Dekorsy
Department of Communications Engineering
University of Bremen, Germany
Email: {haddad, bockelmann, dekorsy}@ant.uni-bremen.de

***Abstract*—In wireless communication, it is essential for the base station (BS) to obtain the downlink channel state information (CSI). In case of the absence of channel reciprocity, the mobile station (MS) needs to report the CSI back to the BS. In mobile multiple input multiple output (MIMO) systems, the CSI feedback overhead grows proportionally with the number of antennas and with the employed bandwidth. Moreover, the channel characteristics change constantly, so the feedback must be reported repeatedly with cautiously designed update intervals depending on how rapidly the channel changes. The increasing CSI overhead becomes a performance bottleneck, therefore it is vital to reduce it while keeping the system performance as good as required. In this paper, we propose a novel method based on designing a dynamical model of a time-varying channel with help of a framework called dynamic mode decomposition (DMD). Reporting the model to the BS gives it the ability to predict the channel state and track its changes over time. Simulation results show that the proposed method can increase the interval duration between the successive feedback updates and thus reduce the average overhead.**

***Index Terms*—MIMO systems, Channel estimation, CSI feedback, Precoding, Time-varying channels, Dynamic Mode Decomposition.**

I. Introduction

Systems employing multiple-antenna techniques are one of the key technologies in the current wireless communication networks. One of the fundamental aspects of MIMO transmission is to ensure an accurate downlink (DL) channel state information (CSI) at the base station (BS). CSI is generally produced at the mobile station (MS) based on the DL channel matrix and then reported to the BS to be used for precoding. The applied precoding scheme depends mainly on the CSI structure. In that regard, having access to the entire DL channel matrix enables the BS to directly use any of the precoding methods, which is essential to reduce interference from other users and hence improve the system performance.

In frequency division duplex (FDD), employing different carrier frequencies in DL and uplink (UL) prevents the usage of channel reciprocity [1]. For time division duplex (TDD), the propagation channel is reciprocal since the same frequency is used in DL and UL. In many cases, the whole channel is considered to be nonreciprocal due to the fact that the transmitter and receiver RF-chains are usually not identical [2]. Accordingly, for both FDD and TDD, the BS cannot count on the UL pilots to obtain the CSI in DL. Thereby, the channel matrix needs first to be estimated at the MS by using DL pilots transmitted from BS. In 5G new radio (NR), the DL pilots are called the CSI reference signal (CSI-RS) as standardized in 3rd generation partnership project (3GPP) [3]. In fact, feeding back the entire channel matrix as observed is very expensive in terms of the UL overhead. Thus, the MS processes the estimated channel to produce a low-dimensional representation that retains the significant properties of the channel matrix. The low-dimensional CSI can be then reported with much less feedback overhead.

The conventional implicit CSI reporting scheme, which is adopted in 3GPP standards [4], makes some assumptions on the BS precoding at the time of feedback. The assumptions are interpreted as several CSI components derived from the estimated channel matrix. Feeding back the CSI components results in less precoding quality since the transmission schemes are limited by the assumptions.

On the other hand, reporting CSI explicitly refers to the feedback of the channel as it is observed by the MS, that can assure high system performance [5]. However, explicit feedback can generate heavy overhead in the UL. That motivates the need to compress the estimated channel matrix at the MS side before sending it back. Various CSI compression techniques have been proposed. Among many works, compressed sensing (CS) [6] is an attractive option. In [7] and [8], the time domain channel sparsity is exploited, so that CS based CSI feedback reduction is used by utilizing orthogonal matched pursuit (OMP), where OMP is a greedy sparsity recovery algorithm to determine the position of the significant channel taps in the time domain. In [9] and [10], the channel matrix is reduced in frequency domain by exploiting the MIMO spatial correlation properties. Principal Component Analysis (PCA) is applied to the channel covariance matrix to derive a compression matrix that is used to obtain the sparse representation of the channel. Another simple method to compress the channel matrix in frequency domain is introduced in [11], where singular value decomposition (SVD) is applied to the channel matrix directly. The CSI feedback consists of the most dominants singular values and their corresponding singular vectors of the decomposed matrix.

In mobile communication, because the terminals and/or scatterers are moving, the channel characteristics change constantly over time. Higher relative velocities result in faster

This work was funded by the German Ministry of Education and Research (BMBF) under grants 16KIS1028 (MOMENTUM) and 16KIS1012 (IRLG).

varying channel characteristics [12]. This leads to a phenomenon called channel aging, i.e., the actual channel differs from the one used for precoding. The effect of channel aging appears first due to the process delay needed to calculate the CSI at the MS and then to perform the precoding at the BS. In both implicit and explicit feedback schemes, the CSI is fed back frequently with intervals. Therefore, the BS uses the reported CSI to perform the precoding within the interval duration until it receives the next update of the CSI. That increases the time delay between the actual channel and the channel used for precoding. Thus, the channel aging effect grows over the the CSI update intervals. Generally, channel aging causes significant degradation in the system performance due to the over-time growing difference between the channel used for precoding and the actual channel at transmission time.

The contribution of this paper is a novel feedback scheme based on analyzing the channel evolution and studying the impact of channel aging. For this purpose, we employ a powerful dimensionality reduction technique called dynamic mode decomposition (DMD) to design a dynamical model of the channel evolution. Besides analyzing the channel changes, the DMD model can also predict the future state of the channel. Feeding back the dynamical model to the BS side makes it possible to predict the channel state. That can reduce the effect of the channel aging and thus improve the precoding performance. In this case, CSI update intervals can be extended and thus the system resources are kept free from overhead for a longer time.

Notations: Throughout this paper, we represent matrices by uppercase boldface letters, column vectors by bold lowercase letters, scalars by italic lowercase letters and numbering by italic uppercase letters. $(.)^H$ denotes the matrix hermitian.

II. System and Channel Models

A. System Model

The system model is depicted in Fig. 1. We consider a MIMO-orthogonal frequency division multiplexing (MIMO-OFDM) system with K subcarriers, N_t Transmit antennas at the BS, and N_r receive antennas at the MS.

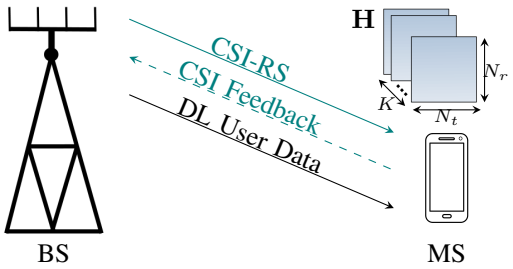

Fig. 1. System Model

MS utilizes the received DL CSI-RS to estimate the channel matrix $\mathbf{H} \in \mathbb{C}^{K \times N_t \times N_r}$. The corresponding CSI is derived from $\mathbf{H}$, then quantized and reported to the BS. The acquired CSI feedback at BS is dequantized and then decompressed to retrieve the channel matrix $\hat{\mathbf{H}}$ that is required to perform the appropriate precoding on the DL user data. However, due to the compression and quantization error, $\hat{\mathbf{H}}$ can deviate from the estimated $\mathbf{H}$, leading to a channel reporting error that depends on the compression degree and the quantization levels. That enables a trade-off relationship between the feedback overhead and the CSI resolution. The received signal on the subcarrier k, $\forall\ k = 1, 2, ..., K$, is defined as:

$$\mathbf{y}_k = \mathbf{H}_k\ \mathbf{W}_k\ \mathbf{s}_k + \mathbf{z}_k \tag{1}$$

where $\mathbf{H}_k \in \mathbb{C}^{N_r \times N_t}$ denotes the channel matrix in frequency domain and $\mathbf{W}_k \in \mathbb{C}^{N_t \times N_r}$ is the corresponding precoding matrix. $\mathbf{y}_k$, $\mathbf{s}_k$, and $\mathbf{z}_k \in \mathbb{C}^{N_r \times 1}$ indicate the received signal, transmitted signal and additive noise, respectively.

B. Time-Varying Channel Model

Due to MS mobility in practical wireless mobile networks, radiated waves suffer from Doppler frequency shift, leading to time-varying multiplicative modifications of the channel in time domain [13]. One parameter used to describe the time-varying channels is the *coherence time* d_c. It indicates the time duration over which the channel is temporally correlated. Essentially, coherence time is inversely proportional to Doppler shift and is defined as:

$$d_c = \frac{c}{2 v f_c} \tag{2}$$

where v, f_c and c denote the MS velocity, the signal carrier frequency and the speed of light, repectively.
The aforementioned channel aging could be quantified by the channel autocorrelation function $R_H(\Delta t)$, as depicted in Fig. 2 [14, Chapter 3]. With increasing the time difference Δt, the channel temporal correlation drops constantly until $\Delta t = d_c$. After this point the correlation could be neglected.

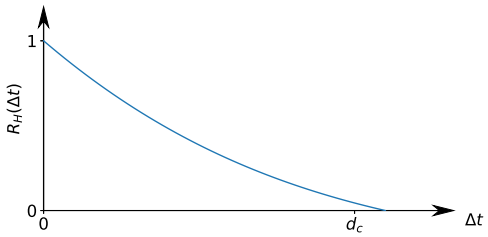

Fig. 2. Channel correlation vs Time difference

Note from (2) that increasing f_c and/or v results in shorter d_c. Fig. 2 implies that shorter d_c leads to faster drop of $R_H(\Delta t)$. That means, the higher the f_c and/or v, the faster changes in the channel.

C. Channel Aging effect on System Model

When considering the properties of time-varying channels, each component of the discussed system model can be redefined as a function of time. In this case, due to the computation delay and CSI reporting intervals, channel aging arises leading to a mismatch between the applied precoding matrix and the actual channel.

As depicted in Fig. 3, after receiving the CSI-RS at time t_1, a process delay d_p is required before starting DL user

data transmission. This delay occurs due to estimating $\mathbf{H}(t_1)$ and finding the corresponding CSI at the MS, as well as for retrieving $\hat{\mathbf{H}}(t_1)$ and designing the precoding matrix $\mathbf{W}(t_1)$ at the BS. The propagation delay is here neglected.
Starting from time $t_2 = t_1 + d_p$, the BS uses $\mathbf{W}(t_1)$ for precoding the transmitted signal until the next CSI feedback is received. The precoding matrix is updated at time $t_3 = t_2 + d_u$, where d_u is the CSI update interval.

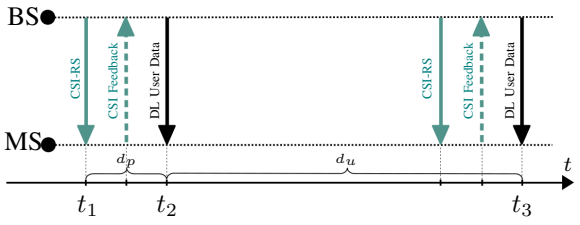

Fig. 3. Process Delay and Update Interval

The received signal at any time t', with $t_2 \leq t' < t_3$, on the subcarrier k is defined as:

$$\mathbf{y}_k(t') = \mathbf{H}_k(t')\ \mathbf{W}_k(t_1)\,\mathbf{s}_k(t') + \mathbf{z}_k(t') \tag{3}$$

The effect of channel aging can be seen clearly in (3) as a mismatch between $\mathbf{W}(t_1)$ and $\mathbf{H}(t')$. Since $\mathbf{W}(t_1)$ is designed based on $\hat{\mathbf{H}}(t_1)$, we quantify this mismatch as the mean square error (MSE) between the reported channel $\hat{\mathbf{H}}(t_1)$ and the actual channel $\mathbf{H}(t')$. The value of the channel MSE indicates the quality of the precoding, i.e, the lower the MSE value the better the preecoding performance. Based on the system requirements, the MSE value must be maintained under some predefined threshold. Note that the channel MSE is affected not only by channel aging but also by the compression and quantization error. In this paper, we address only the error caused by the channel aging effect, as discussed later.

Based on the discussion in Fig. 2, it is understood that increasing Δt reduces the channel correlation and thus increases the channel MSE. In connection with Fig. 3, since $\Delta t = t' - t_1$ keeps growing within d_p, the value of MSE keeps increasing over time up to the next update at t_3. Reducing the process delay and update intervals can be beneficial to prevent the MSE value from growing over the system requirements. d_p can be shrunk by employing more powerful hardware, which is an expensive solution and works only during d_p. Whereas d_u can be reduced by updating CSI more frequently, which results in higher average CSI overhead. The idea here is to find a method to reduce the error caused by channel aging and keep the MSE value sufficiently low as long as possible. In this case, d_u can be extended and thus the channel resources can be retained free from the CSI overhead for a longer time.

Our proposed solution is a new technique that can cope with the effect of the channel aging within the coherence time d_c by exploiting the channel temporal correlation properties. The reported CSI contains information about the channel evolution that allows the BS to predict the future state of the channel and thus track the channel changes in the time domain. Then, the channel aging effect is eliminated since channel MSE is calculated between the predicted channel $\hat{\mathbf{H}}(t')$ and the actual channel $\mathbf{H}(t')$. However, performing such prediction technique could add a prediction error, affecting the channel MSE. Moreover, since this kind of error is accumulative, the MSE value will also increase over time. Simulation results show that the prediction error is considerably lower than the channel aging error, which makes the proposed solution preferable in terms of reducing the MSE.

D. Aperiodic Feedback

Based on the previous discussion, the appropriate update interval must be determined considering the channel MSE. Because the MSE value grows over time, d_c can be extended to the maximum value that corresponds to the maximum allowed MSE, based on the system requirements. Assuming the MS is able to measure the MSE and compare it to some given threshold γ, a simple feedback scheme could be: if MSE $\geq \gamma$, then report back a new CSI. Furthermore, MSE measurement at the MS is easily enabled by utilizing the CSI feedback. The MS can reproduce the channel matrix. It is denoted as $\hat{\mathbf{H}}(t_1)$ in case of no channel prediction or $\hat{\mathbf{H}}(t')$ in case of channel prediction. The MSE could be obtained by comparing the reproduced channel to the estimated channel $\mathbf{H}(t')$.
Choosing the value of γ plays a trade-off role between the MSE value, i.e., the system performance and the CSI feedback intervals, i.e., the overhead.

III. Explicit CSI Feedback

In this section, we concisely discuss two fundamentally different explicit CSI feedback schemes that are needed for comparison purposes in the simulation section. The first scheme is CS based CSI feedback by utilizing the OMP. It is used to find the sparse representation in time domain [7] and [8]. Whereas the second scheme is performed directly in frequency domain by utilizing the SVD that is applied to obtain a low-dimensional CSI [11].

A. OMP based Explicit Feedback

The traditional CS method is used for dimensionality reduction. It assumes the concerned data to be sparse in some basis. After applying the appropriate transformation, the sparse data can be compressed by considering only the nonzero elements with their locations [6].
In case of compressing the channel matrix, the MS can estimate the channel in frequency domain $\mathbf{H}(t)$, which is not sparse. However, the corresponding channel in time domain $\mathbf{G}(t) \in \mathbb{C}^{L \times N_t \times N_r}$ is sparse over the first dimension L. The relationship between $\mathbf{H}(t)$ and $\mathbf{G}(t)$ can be defined as applying the Fourier transformation on time domain channel resulting in the corresponding channel on frequency domain:

$$\mathbf{H}(t) = \mathbf{F}\mathbf{G}(t) \tag{4}$$

where $\mathbf{F} \in \mathbb{C}^{K \times L}$ is the DFT matrix and L is the Fourier transform size. $K < L$ since only a portion of the spectrum is utilized and the rest is restrained to comply with standardized spectral masks. Since (4) is underdetermined, $\mathbf{G}(t)$ cannot be

calculated directly by taking the inverse of $\mathbf{F}$. Thus, a search algorithm is needed to detect the sparse solution.

In [7] and [8], the OMP algorithm is utilized to find the most sparse solution. At the MS, OMP runs a greedy search over a range of length $D < L$ to detect the value and location of the most powerful nonzero element, where D is chosen equal to the length of the cyclic prefix. This search step is repeated several times C with considering the previously detected elements. Since each search step results in one element, the final output is C elements.

The number of search steps C can be adjusted as a trade-off between the computing time and output resolution. Hereby, we denote the solution based on OMP output as $\hat{\mathbf{G}}(t)$. The values and locations of the nonzero elements are fed back. At the BS side, $\hat{\mathbf{G}}(t)$ is reconstructed and used (4) to obtain the corresponding channel in frequency domain $\hat{\mathbf{H}}(t)$.

B. SVD based Explicit Feedback

The SVD method can be applied at the MS directly on the channel in frequency domain. Since SVD is used with 2D matrices, the 3D channel matrix $\mathbf{H}(t)$ can be split into N_r matrices, each of size $K \times N_t$. Moreover, to reduce the SVD input, the correlation in frequency domain can be exploited by dividing the dimension K into B subbands, so that each subband contains $\frac{K}{B}$ subcarriers. The first subcarrier in each subband is used to build the SVD input $\bar{\mathbf{H}}_{n_r}(t) \in \mathbb{C}^{B \times N_t}$ $\forall\ n_r = 1, 2, ..., N_r$.

Then SVD is performed separately on each $\bar{\mathbf{H}}_{n_r}(t)$ as:

$$\bar{\mathbf{H}}_{n_r}(t) = \mathbf{U}_{n_r}(t)\mathbf{\Sigma}_{n_r}(t)\mathbf{V}^H_{n_r}(t) \tag{5}$$

where $\mathbf{U}_{n_r}(t) \in \mathbb{C}^{B \times B}$ and $\mathbf{V}_{n_r}(t) \in \mathbb{C}^{N_t \times N_t}$ are the left and right singular vectors matrices, respectively, and $\mathbf{\Sigma}_{n_r}(t) \in \mathbb{C}^{B \times N_t}$ is a diagonal matrix with singular values that are sorted in a descending manner.

Due to the nature of SVD, it can be truncated by setting all but the first r_{svd} largest singular values equal to zero, where r_{svd} denotes the SVD rank. That results in truncated components $\hat{\mathbf{U}}_{n_r}(t) \in \mathbb{C}^{B \times r_{svd}}$, $\hat{\mathbf{\Sigma}}_{n_r}(t) \in \mathbb{C}^{r_{svd} \times r_{svd}}$ and $\hat{\mathbf{V}}_{n_r}(t) \in \mathbb{C}^{N_t \times r_{svd}}$.

The singular values in $\hat{\mathbf{\Sigma}}_{n_r}(t)$ can be left or right multiplied by $\hat{\mathbf{U}}_{n_r}(t)$ or $\hat{\mathbf{V}}_{n_r}(t)$, respectively, before feeding back. At the BS, the channel can be recomposed as:

$$\hat{\bar{\mathbf{H}}}_{n_r}(t) = \hat{\mathbf{U}}_{n_r}(t)\hat{\mathbf{\Sigma}}_{n_r}(t)\hat{\mathbf{V}}^H_{n_r}(t) \tag{6}$$

Each subcarrier in $\hat{\bar{\mathbf{H}}}_{n_r}(t)$ is repeated $\frac{K}{B}$ times to obtain $\hat{\mathbf{H}}_{n_r}(t)$. Then, the resulting N_r matrices are appended to obtain $\hat{\mathbf{H}}(t)$.

Choosing r_{svd} properly can reduce the CSI feedback considerably while maintaining the approximation $\hat{\mathbf{H}}(t) \approx \mathbf{H}(t)$ since the most power is in the first singular values.

C. Explicit CSI Feedback scheme

The proposed aperiodic explicit CSI Feedback scheme is summarized in Table I. It could be performed by applying either OMP or SVD to compress the estimated channel.

TABLE I
EXPLICIT CSI FEEDBACK SCHEME

Step 0: Input γ.
Initialize $m = 1$, *bool* =True.
Step 1: Estimate the channel $\mathbf{H}(t_m)$.
Step 2: Compress and Quantize to obtain CSI.
- if *bool* =True: Feed back CSI.

———MS checking the condition for next feedback———
Step 4: Decompress and Dequantize CSI to obtain $\hat{\mathbf{H}}(t_m)$.
Step 5: Calculate MSE between $\mathbf{H}(t_1)$ and $\hat{\mathbf{H}}(t_m)$.
- if MSE$< \gamma$: *bool* =False
- else: *bool* =True. $m = 0$

Step 6: $m = m + 1$, goto **Step 1**

IV. CHANNEL MODELING WITH DMD

In this section we explain the fundamental concept of the DMD method and how it is implemented in a time-varying channel to reduce the average CSI overhead.

A. Dynamic Mode Decomposition

DMD [14] is an equation-free data-driven method capable of providing an accurate decomposition of a complex system into spatiotemporal coherent structures that may be used for short time future state prediction. The method relies on collecting M observed snapshot data $\mathbf{X}(t_m)$ from a dynamical system at a number of times t_m, where $m = 1, 2, ..., M$. Each snapshot data is reshaped into a column vector of length N, i.e., $\mathbf{x}(t_m) \in \mathbb{C}^{N \times 1}$. The collected snapshots are then arranged into two large data matrices:

$$\begin{aligned} \mathbf{X} &= [\mathbf{x}(t_1)\ \mathbf{x}(t_2)\ ...\ \mathbf{x}(t_{M-1})] \\ \mathbf{X}' &= [\mathbf{x}(t_2)\ \mathbf{x}(t_3)\ ...\ \mathbf{x}(t_M)] \end{aligned} \tag{7}$$

where $\mathbf{X}$ and $\mathbf{X}' \in \mathbb{C}^{N \times M-1}$. DMD calculates the best-fit linear dynamical system, even if the data snapshots may be captured from a nonlinear system. It finds linear approximation that describes how the matrix $\mathbf{X}'$ advances from $\mathbf{X}$ as:

$$\mathbf{X}' \approx \mathbf{A}\mathbf{X} \tag{8}$$

where $\mathbf{A} \in \mathbb{C}^{N \times N}$ is an approximating linear operator chosen to minimize the Frobenius norm of the error $\|\mathbf{X}' - \mathbf{A}\mathbf{X}\|_F$ by utilizing the standard linear regression.

In practice, when data dimension N is large, the matrix $\mathbf{A}$ may be intractable to analyze directly. Therefore, instead of solving (8) for $\mathbf{A}$ directly, DMD utilizes a spatial dimensionality-reduction technique called proper orthogonal decomposition (POD). The collected data are projected onto a low-rank subspace defined by at most $M - 1$ POD modes and then solved for a low-dimensional linear operator. This process can calculate the eigendecomposition of the matrix $\mathbf{A}$ without ever explicitly computing $\mathbf{A}$ [14]. The solution yields eigenvectors $\boldsymbol{\phi}_m \in \mathbb{C}^{N \times 1}$ and eigenvalues $\lambda_m \in \mathbb{C}$ of the mapping operator $\mathbf{A}$ which are called DMD modes and dynamics, respectively. The DMD modes represent coherent space-frequency structures, whereas the DMD dynamics describe how the corresponding modes evolve.

The eigendecomposition solution can be recomposed to represent the data at any time m as:

$$\mathbf{x}(t_m) = \sum_{j=1}^{r_{dmd}} \boldsymbol{\phi}_j \lambda_j^m b_j \tag{9}$$

where each b_j denotes the initial amplitude of the corresponding mode $\boldsymbol{\phi}_j$, whereas r_{dmd} is the DMD rank. r_{dmd} indicates the number of used eigendecompositions, i.e., eigenvalues and eigenvectors with $1 \leqslant r_{dmd} \leqslant M$. The higher the value of r_{dmd}, the better the resolution of $\mathbf{x}(t_m)$. However, important to mention that the generated eigendecompositions are sorted in descending order from the most significant. Accordingly, it may be sufficient to take only first r_{dmd} modes and dynamics out of the entire available M to ensure an adequate resolution of any recomposed $\mathbf{x}(t_m)$.
For prediction's sake, formula (9) can be run forward by taking times $t_{m'}$ in the future, i.e., $m' = M+1, M+2, \ldots$.

B. Dynamical Model CSI Feedback

In this subsection, we discuss how to employ the aforementioned DMD in a practical wireless system. Due to the temporal correlation properties of a time-varying channel in mobile wireless communication, the evolved channel can be seen as a dynamical system. DMD could be applied to generate a dynamical model that describes the channel changes. The model consists of modes and dynamics which can be used to perform future state prediction of the channel.
The last M estimated channel matrices $\mathbf{H}(t_m)$, where $m = 1, 2, ..., M$, can be saved at the MS to be used as input data snapshots to the DMD algorithm. Each matrix snapshot is first reshaped into a column vector $\mathbf{h}(t_m) \in \mathbb{C}^{N \times 1}$ as $N = KN_tN_r$. Thereafter, the channel vectors are stacked into two big matrices as in (7). The resulting $\mathbf{X}$ and $\mathbf{X}'$ can be used as input to the DMD algorithm to produce the corresponding dynamical model, i.e., eigenvectors $\boldsymbol{\phi}_m$ and eigenvalues λ_m of the linear operator $\mathbf{A}$ that fulfills the approximation $\mathbf{X}' \approx \mathbf{AX}$. The designed dynamical model must be fed back to the BS.

In order to calculate the feedback overhead, the size of the DMD model could be calculated from (9) by summing only the sizes of modes and dynamics. The initial amplitude size should not be counted since b_j could be multiplied by $\boldsymbol{\phi}_j$. Each mode $\boldsymbol{\phi}_j$ is a vector of length N coefficients while each dynamic λ_j is one coefficient. Because r_{dmd} can be chosen up to M, the maximum size of the dynamical model is $(N+1)M$ coefficients. This size is too big and also larger than the channel $\mathbf{h}(t)$ size. Thus, it needs to be compressed. Because the eigendecompositions are sorted descendingly, we can reduce the number of needed modes and dynamics considerably while keeping the most of the power after recomposition. Accordingly, the size of the dynamical model could be shrunk to $(N+1)r_{dmd}$.

Further compression can be performed by reducing the size of each selected mode. Reducing the mode size relies on the fact that the mode coefficients for the dominant POD modes are sparse in the frequency domain [14]. Thus, applying Fourier transformation to the modes results in sparse output.

1) Example of mode compression: Fig. 4 depicts an example of applying Fourier transformation to the first mode $\boldsymbol{\phi}_1$ of a channel dynamical model. For simplification, we consider single input single output (SISO) with $K = 660$ subcarriers. In (a), the mode is depicted in time domain before compression. Note in (b) how sparse the mode is in frequency domain. Only some elements N_z contain the most of the power. In (c) we take $N_z = 8$ and apply the inverse Fourier transformation to retrieve the mode in time domain (d).
To evaluate the reduction performance, we calculate the size of the mode in bits before and after compression. The quantization is performed in amplitude and phase with $N_b = 8$ bits for each complex coefficient. The amplitude is quantized in a differential manner so that the strongest coefficient amplitude is set to 1 as a reference amplitude and then quantized to $Am = 3$ bits. Whereas the phase of each coefficient is quantized using $Ph = 5$ bits, i.e., 32-PSK points. The locations of the nonzero elements are defined as integer values within a range of length N, thus, they can be measured with $N_z\lceil log_2(N) \rceil$ bits.
Accordingly, the size of the compressed mode is calculated with $N_z(N_b + \lceil log_2(N) \rceil) = 144$ bit. Whereas, the mode size without compression is $N_b \times N = 5280$ bit.

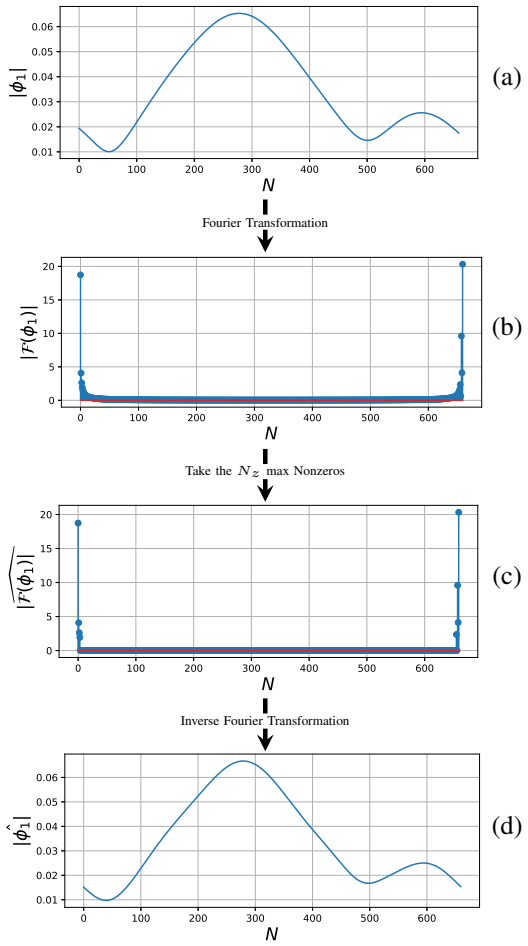

Fig. 4. Mode Compression

The CSI overhead of the dynamical model comprises r_{dmd} compressed modes with their dynamics. At the BS, the reported CSI is first dequantized and decompressed to retrieve the dynamical model. By applying (9), the channels $\hat{\mathbf{h}}(t_m)$ can be obtained. Note that $\hat{\mathbf{h}}(t_m)$ deviate from $\mathbf{h}(t_m)$ due to compression and quantization error. The values of the parameters r_{dmd}, N_z and N_b play a trade-off role between the overhead and the CSI quality.

C. Dynamical Model CSI Feedback scheme

The proposed aperiodic dynamical model CSI feedback scheme is summarized in Table II. This scheme depends on collected data from the past. Therefore, the first CSI feedback can be generated after a time delay. This time is needed at the MS to collect the estimated channels $\mathbf{H}(t_m)$, with $m = 1, 2, ..., M$. This delay occurs only once when starting up the MS. **Step 0** represent the starting up process.

TABLE II
DYNAMICAL MODEL CSI FEEDBACK SCHEME

Step 0: Input M, γ, r_{dmd}
Initialize $m = 1$, $m' = M + 1$, $\dot{\mathbf{H}} = \mathbf{0}$
while $m \leq M$: repeat
- Estimate the channel $\mathbf{H}(t_m)$.
- Reshape $\mathbf{H}(t_m)$ to vector $\mathbf{h}(t_m)$ and stack in $\dot{\mathbf{H}}$.
- $m = m + 1$

Step 1: Remove the channels in $\dot{\mathbf{H}}$ older than M.
Step 2: Construct $\mathbf{X}$ and $\mathbf{X}'$ from $\dot{\mathbf{H}}$.
Step 3: Apply DMD on $\mathbf{X}$ and $\mathbf{X}'$ to obtain the modes $\mathbf{\Phi}$ and dynamics $\mathbf{\Lambda}$.
Step 4: Compress and Quantize the r_{dmd} most dominant modes in $\mathbf{\Phi}$ and obtain CSI.
Step 5: Feed back CSI.
——MS checking the condition for next feedback——
Step 6: Decompress and Dequantize CSI.
Step 7: Predict $\hat{\mathbf{H}}(t_{m'})$.
Step 8: Estimate the channel $\mathbf{H}(t_{m'})$.
Step 9: Reshape $\mathbf{H}(t_{m'})$ to column vector $\mathbf{h}(t_{m'})$ and stack in $\dot{\mathbf{H}}$.
Step 10: Calculate MSE between $\mathbf{H}(t_{m'})$ and $\hat{\mathbf{H}}(t_{m'})$.
- if MSE$(t_{m'}) < \gamma$: $m' = m' + 1$, goto **Step 7**
- else: $m' = M + 1$, goto **Step 1**

V. SIMULATION RESULTS

In this section, we perform numerical simulations to evaluate the performance of the dynamical model CSI feedback scheme and compare it to the explicit CSI feedback schemes. For the simulations, we employ Heterogenous Radio Mobile Simulator (HermesPy) [15] to generate the channel coefficients. System parameters are enumerated in Table III.
The simulation is run under two conditions, perfect and imperfect channel estimation.

A. Perfect Channel Estimation

For now, the channel estimation at the MS is considered to be perfect. We compare the channel MSE evolution for two CSI feedback schemes. One based on dynamical model feedback (DM-FB) and the other based on explicit feedback (E-FB). For the explicit feedback, it makes no difference to apply OMP or SVD, since both just compress the estimated channel

TABLE III
SIMULATION PARAMETERS

System Parameters	Value
Channel model	COST 259 [16]
Channel generator	HermesPy
Carrier frequency f_c	2 GHz
MS velocity v	5 Km/h
Number of BS antenna N_t	4
Number of MS antenna N_r	4
System bandwidth	10 MHz
Subcarrier spacing	15 KHz
Number of subcarriers K	660
DFT size L	1024
Collected data duration M	25 ms
Quantization Am/Ph	3/5 bit
Channel estimating error	AWGN
CSI feedback	Aperiodic
CSI update threshold γ	-5dB
DMD Parameters	**Value**
DMD rank r_{dmd}	2
tlsq_Rank r_{tlsq}	2
OMP Parameters	**Value**
Search range D	256
Stopping condition C	10
SVD Parameters	**Value**
SVD Rank r_{svd}	2
Number of subblocks B	22

and feed it back. Then, the BS uses the reported channel within the entire update interval d_u. To focus the comparison on the MSE evolution we set the schemes parameters such that the MSE at the reporting time is equal for DM-FB and E-FB. Therefore, the DMD parameters are chosen $r_{dmd} = 2$, $M = 350 \triangleq 25\,\text{ms}$ and m' up to $1050 \triangleq 75\,\text{ms}$. Whereas, the OMP parameters are $D = 256$ and $C = 10$, or the SVD parameters are $r_{svd} = 2$ and $B = 22$. As seen in Fig. 5, the MSE value at $t = 0\,\text{ms}$ is almost the same for DM-FB and E-FB and is not equal to zero because of the compression and quantization error. Over time, The MSE grows worse for both schemes. However, it is obvious that the slope of the DM-FB is much lower than the E-FB. this shows that the accumulative prediction error is much lower than the channel aging error. According to (2), we calculate $d_c \approx 56\,\text{ms}$. Note in the figure that the MSE value grows steadily over d_c.

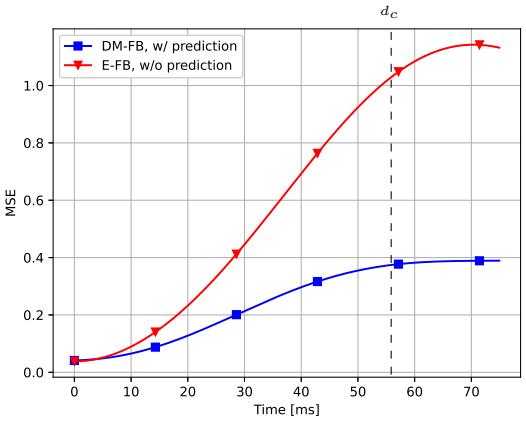

Fig. 5. Channel MSE evolution

To evaluate the CSI feedback overhead reduction, we consider the aperiodic feedback scheme. The threshold is chosen arbitrary as $\gamma = 0.32 \approx -5\,\text{dB}$. For each of the discussed methods, DM-FB using DMD and E-FB using OPM snd SVD, the overhead is calculated and listed in the Table IV. We notice that the transmitted CSI feedback for DMD is higher. However, looking at the average overhead per second we notice that DMD generates less overhead since it feeds back less frequently than the other explicit techniques. By applying DMD we save about $8\,\text{Kbit}$ compared to OMP and $21\,\text{Kbit}$ compared to SVD every second.

TABLE IV
CSI OVERHEAD VALUES IN BITS

	DMD	**OMP**	**SVD**
at once	2144	1360	1664
avr (1s)	51381.53	59646.23	72476.25

B. Imperfect Channel Estimation

Since the channel estimation error is not accumulative, it affects the MSE at the reporting time and not the MSE evolution. Therefore, we focus the comparison here on the MSE at the reporting time. In the simulation we consider the estimation error as AWGN and represent it as SNR value.
DMD offers a variant called total least-squares DMD (tlsq-DMD). It is able to handle the noisy input data to mitigate the noise effect, i.e., estimation error, by applying the total least-squares algorithm [14], which is an extension of the standard SVD-based least-squares regression. For the aperiodic feedback decision, the threshold is again chosen as 0.32.

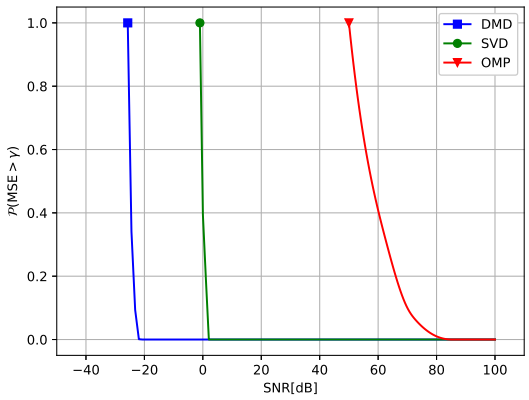

Fig. 6. SNR vs $\mathcal{P}(\text{MSE} > \gamma)$ with $\gamma = 0.32$

In Fig. 6, we compare the quality of the reported CSI at the current time of the three discussed feedback methods, based on DMD, OMP and SVD. The y-axis represents the probability that the MSE is higher than the threshold γ, i.e., the probability that the CSI feedback fails to fulfill the system requirements. Whereas the x-axis shows the SNR that represents the estimation error.
The probability that MSE > 0.32 starts to degrade when the SNR value is lower than $-22\,\text{dB}$, $2\,\text{dB}$ and $80\,\text{dB}$, when applying DMD, SVD and OMP, respectively. Therefore, applying DMD provide the most robust performance against the estimation error compared to other schemes.

VI. CONCLUSION

In this paper, we discussed a CSI feedback scheme based on reporting a dynamical model that describes the channel evolution. The proposed method exploits the temporal correlation properties of the channel in order to mitigate the channel aging effect. The designed model is able to predict the future state of the channel and hence to track the channel changes. Therefore, the CSI update intervals could be increased.
Even though the dynamical model can be compressed before feeding back, its size is larger than other proposed E-FB size. However, DM-FB ensures longer CSI update intervals and consequently less average CSI feedback overhead.
Moreover, in practice when the channel estimation is imperfect, the proposed DM-FB utilizes the total least-squares algorithm. It shows impressive robust performance against the estimation error compared to other E-FB using OMP or SVD.

REFERENCES

[1] T. Laas, J. A. Nossek, S. Bazzi, and W. Xu, "On reciprocity in physically consistent tdd systems with coupled antennas," IEEE Transactions on Wireless Communications, vol. 19, no. 10, pp. 6440–6453, 2020.
[2] H. Asplund, D. Astely, P. von Butovitsch, T. Chapman, M. Frenne, F. Ghasemzadeh, M. Hagström, B. Hogan, G. Jongren, J. Karlsson, et al., Advanced Antenna Systems for 5G Network Deployments: Bridging the Gap Between Theory and Practice. Academic Press, 2020.
[3] "ETSI TS 138 211." https://www.etsi.org/deliver/etsits/138200138299/138211/16.02.0060/ts138211v160200p.pdf.
[4] "ETSI TS 138 214." https://www.etsi.org/deliver/etsits/138200138299/138214/16.02.0060/ts138214v160200p.pdf.
[5] B. Clerckx, G. Kim, J. Choi, and Y.-J. Hong, "Explicit vs. implicit feedback for su and mu-mimo," in 2010 IEEE Global Telecommunications Conference GLOBECOM 2010, pp. 1–5, IEEE, 2010.
[6] R. G. Baraniuk, "Compressive sensing [lecture notes]," IEEE signal processing magazine, vol. 24, no. 4, pp. 118–121, 2007.
[7] Y. Li and R. Song, "Novel scheme of csi feedback compression for multi-user mimo-ofdm system," Procedia Engineering, vol. 29, pp. 3631–3635, 2012.
[8] R. Ahmed, E. Visotsky, and T. Wild, "Explicit csi feedback design for 5g new radio phase ii," in WSA 2018; 22nd International ITG Workshop on Smart Antennas, pp. 1–5, VDE, 2018.
[9] A. Ge, T. Zhang, Z. Hu, and Z. Zeng, "Principal component analysis based limited feedback scheme for massive mimo systems," in 2015 IEEE 26th Annual International Symposium on Personal, Indoor, and Mobile Radio Communications (PIMRC), pp. 326–331, IEEE, 2015.
[10] J. Joung, E. Kurniawan, and S. Sun, "Principal component analysis (pca)-based massive-mimo channel feedback," arXiv preprint arXiv:1512.05068, 2015.
[11] R. Ahmed, K. Jayasinghe, and T. Wild, "Comparison of explicit csi feedback schemes for 5g new radio," in 2019 IEEE 89th Vehicular Technology Conference (VTC2019-Spring), pp. 1–5, IEEE, 2019.
[12] G. Matz and F. Hlawatsch, "Time-varying communication channels: Fundamentals, recent developments, and open problems," in 2006 14th European Signal Processing Conference, pp. 1–5, IEEE, 2006.
[13] G. Matz and F. Hlawatsch, "Fundamentals of time-varying communication channels," in Wireless communications over rapidly time-varying channels, pp. 1–63, Elsevier, 2011.
[14] J. N. Kutz, S. L. Brunton, B. W. Brunton, and J. L. Proctor, Dynamic mode decomposition: data-driven modeling of complex systems. SIAM, 2016.
[15] "HermesPy." https://www.barkhauseninstitut.org/en/results/hermespy.
[16] "ETSI TR 125 943." https://www.etsi.org/deliver/etsitr/125900125999/125943/06.00.0060/tr125943v060000p.pdf.